

# EARLY PROGRESS ON ADDITIVE MANUFACTURING OF NUCLEAR FUEL MATERIALS

A. BERGERON, J.B. CRIGGER

*Fuel Development Branch, Canadian Nuclear Laboratories  
286 Plant Rd., Chalk River, Ontario, K0J1J0- Canada*

## ABSTRACT

Additive manufacturing of thorium dioxide has been investigated using a commercially available stereolithography-based 3D printer and photopolymer resin. Three-dimensional thorium dioxide objects have been printed with good dimensional accuracy. High-density thorium dioxide parts (>90% theoretical density) were achieved by sintering the 3D-printed parts. Despite significant shrinkage, the overall shape of the objects was maintained during sintering with slight distortion. Additive manufacturing is seen to have potential application for advanced nuclear fuel concepts with complex geometries.

## 1. Introduction

Advanced nuclear fuel concepts may offer better performance, increased safety margins, and greater accident tolerance. Often these concepts are based on advanced materials, have inhomogeneous structures, or have complex geometries. Many of these next generation fuels cannot be manufactured via the conventional processes applied to traditional ceramic nuclear fuels. Therefore, new methods are required to manufacture these fuels.

One such manufacturing method is additive manufacturing, e.g. 3D printing. The term additive manufacturing encompasses a wide variety of technologies used to build three-dimensional objects by adding layer upon layer of material. In 3D printing, models of an object are developed using computer-aided design software (CAD). Additional software is used to slice the model into individual layers of a defined height for printing and to develop the set of instructions required for a machine to deposit the material of each layer. These technologies have been applied to a variety of materials including plastics, metals, composites and ceramics [1]. New developments in additive manufacturing using nuclear fuel materials open the doors for innovative fuel designs with complex geometries that could not have otherwise been manufactured using conventional methods [2].

In this study, fabrication trials of thorium dioxide objects using stereolithography at Canadian Nuclear Laboratories (CNL) are reported. Thorium dioxide was chosen as the first fuel material to print (as opposed to the more commonly employed uranium dioxide) due to its similar optical properties to materials such as alumina and zirconia, which have been fabricated using similar stereolithography-based methods [3].

## 2. Materials and Methods

Stereolithography was employed in this study which uses an ultraviolet laser to selectively polymerize a photosensitive liquid resin [4]. A build platform is lowered into a vat of resin, and the laser traces the design of each layer of the object through a window at the bottom of the vat. The first layer adheres to the build platform and each successive layer adheres to the previous one as the build platform indexes. A schematic for the process is provided in Figure 1.

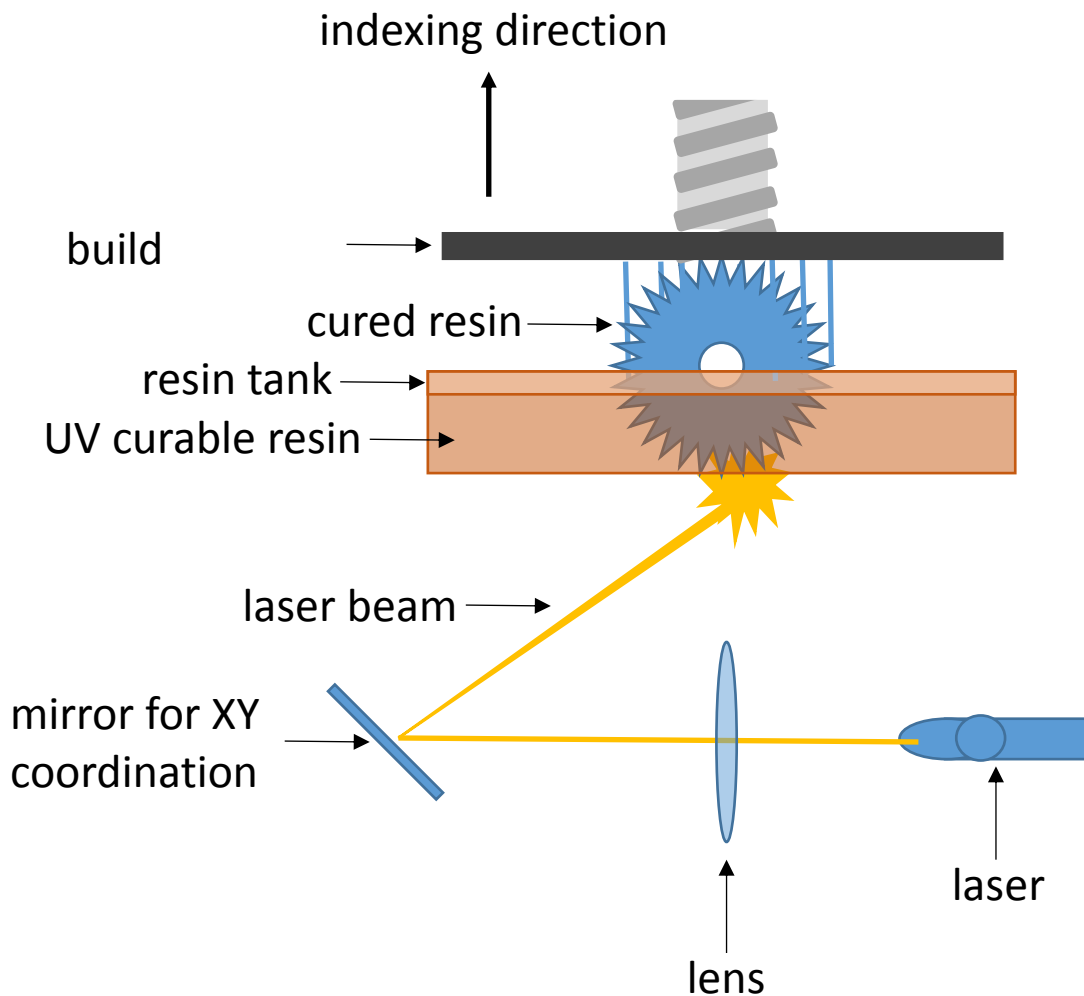


Fig 1: Schematic of stereolithography process

A commercially available 3D printer was used. The 3D printer uses a 405 nm violet laser with a power of 250 mW to cure the photopolymer resin. During experimental trials a layer thickness of 50 microns was used.

Commercially available photopolymer resin was used with the 3D printer. The material is a development resin base that can be combined with solid powders to create a novel 3D printable resin. It contains a mixture of alkoxyated pentaerythritol tetraacrylate, 2-[[[(butylamino)carbonyl]oxy]ethyl acrylate, di(trimethylolpropane) tetraacrylate, dibutyltin dilaurate, and diphenyl(2,4,6-trimethylbenzoyl)phosphine oxide proprietary to the manufacturer. In this study, the resin was combined with thorium dioxide powder.

The particle size distribution of the thorium dioxide powder was measured using a particle size analyzer with and without the use of an in-line ultrasonic probe to break up agglomerates. The mean particle sizes were 2.0  $\mu\text{m}$  and 7.3  $\mu\text{m}$ , respectively. The surface area of the powder was measured using a surface area/pore size analyzer as 6.865  $\text{m}^2/\text{g}$ . A scanning electron microscopy image of the powder is provided in Figure 2 demonstrating the spherical shape of granules. Impurities analysis of the starting powder is provided later. Prior to mixing the thorium dioxide with the photopolymer resin, the powder was sieved through a 150 micron mesh screen to remove any large powder agglomerates. A Turbula shaker/mixer was used to mix the resin and powder in a ratio of approximately 3:10 by weight. Before printing trials, the resin mixture was agitated in the Turbula to re-suspend any powder particles that had settled over time.

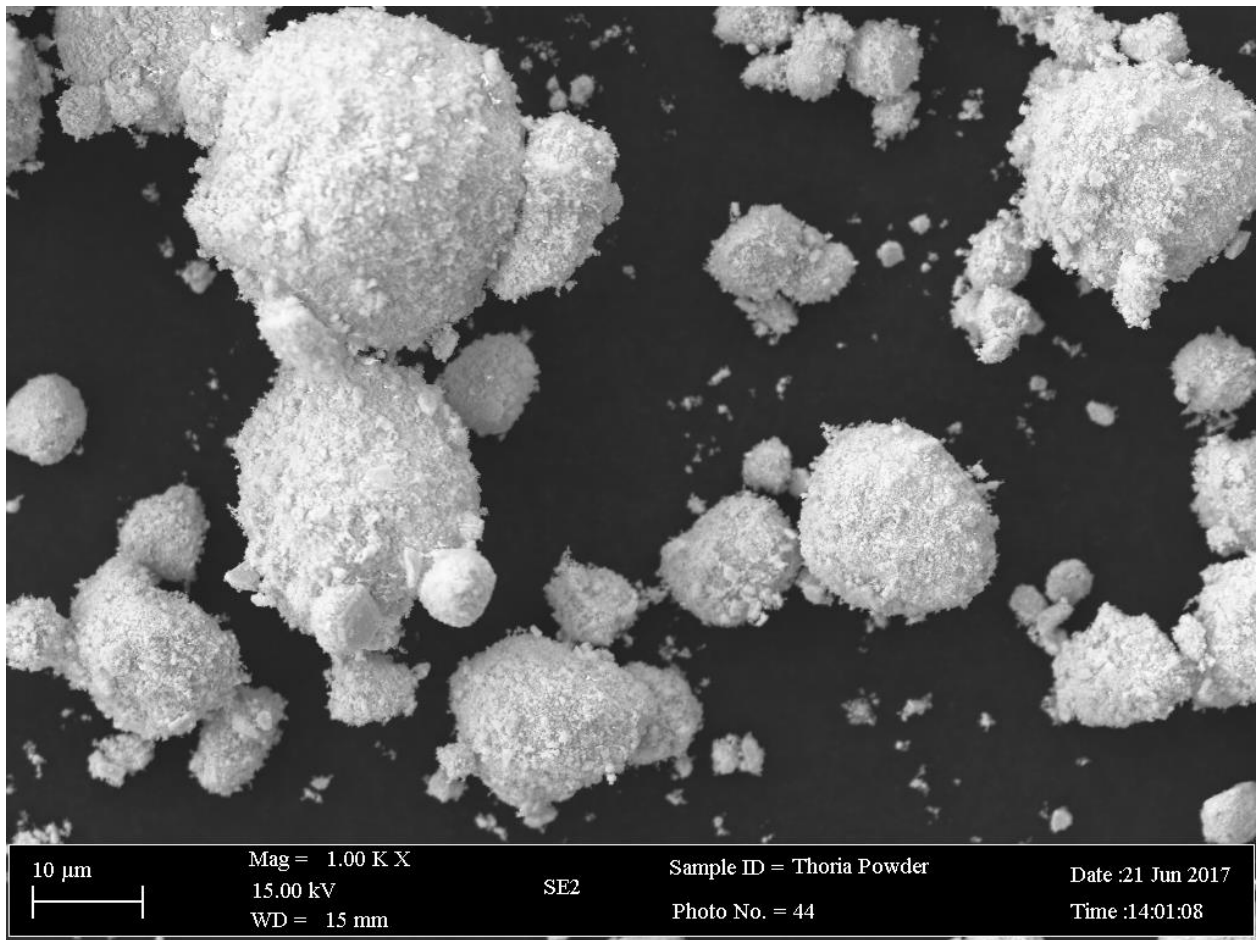


Fig 2: SEM Image of Starting Thoria Powder showing Spherical Granules

The parts that were fabricated using the 3D printer were 1 cm<sup>3</sup> hollow cubes. This shape was chosen because it cannot be made using conventional powder pressing methods and because it is easy to measure the principal dimensions using calipers. Two identical parts were printed at once and total printing time was approximately 3.5 hours. The 3D rendering of the parts is shown in Figure 3. Also pictured is the base and support structure of the cubes. The base adhered to the build platform and the support structure connected the part to the base, providing reinforcement. During printing, the part was inverted and suspended from the build platform.

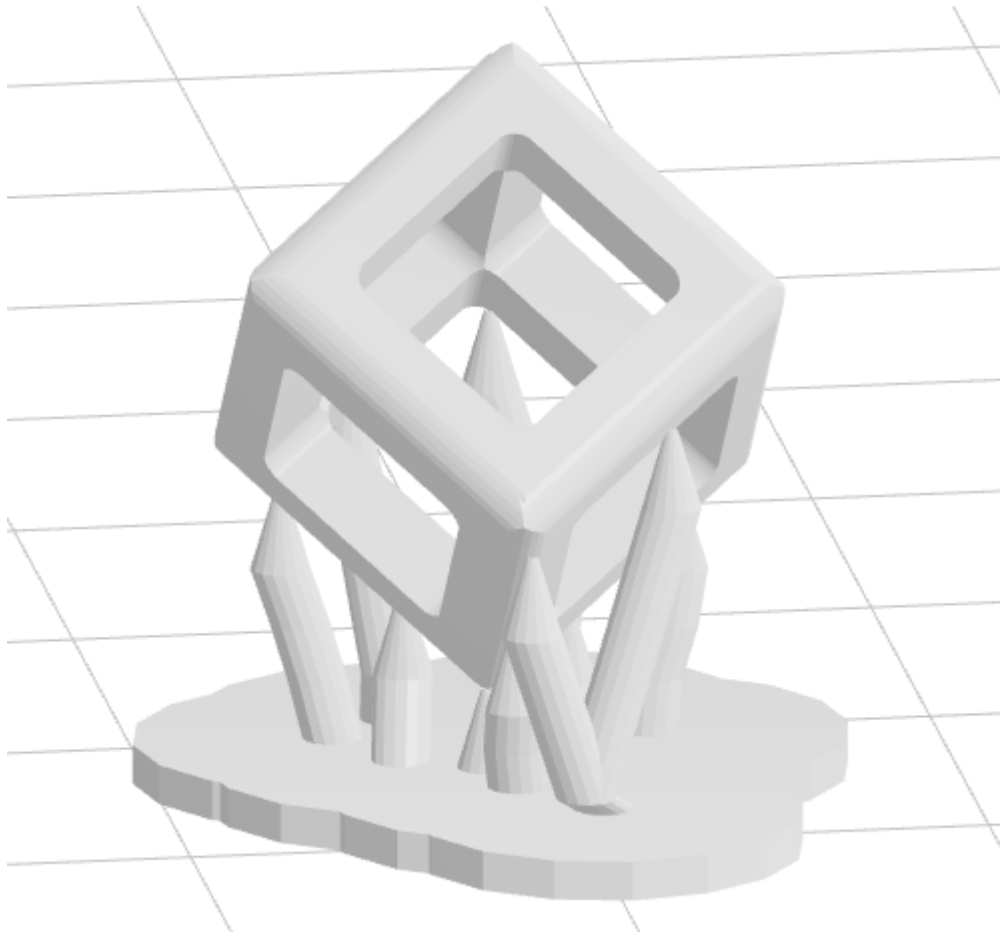


Fig 3: 3D Model of 1 cm<sup>3</sup> Hollow Cube with Support Structure (not to scale)

Post printing, parts were washed in isopropyl alcohol to remove any excess resin, and allowed to air dry. The cubes were placed in a UV light box overnight for post-curing. The support structure of the cubes was then cut away.

To achieve high density parts, the cubes were sintered in air at 1700°C for 2 hours in a high temperature box furnace. The sintering cycle included a resin burnout step at lower temperatures prior to heating to sintering temperatures and is depicted in Figure 4. The support structures that had been cut away from the cubes were sintered with the cubes so that the material could be analyzed for impurities. Impurity content in the sintered material was compared with that measured in the starting thorium dioxide powder. The resin contained a mixture of hydrocarbon monomers with a catalyst containing tin (Sn) and a photoinitiator (to initiate polymerization of the resin on exposure to UV light) containing phosphorus (P). The concentrations of carbon and tin were measured to determine the effectiveness of resin burnout. Carbon content was measured using a carbon and sulfur determinator. Tin and other impurities were measured using inductively coupled plasma mass spectrometry (ICP-MS).

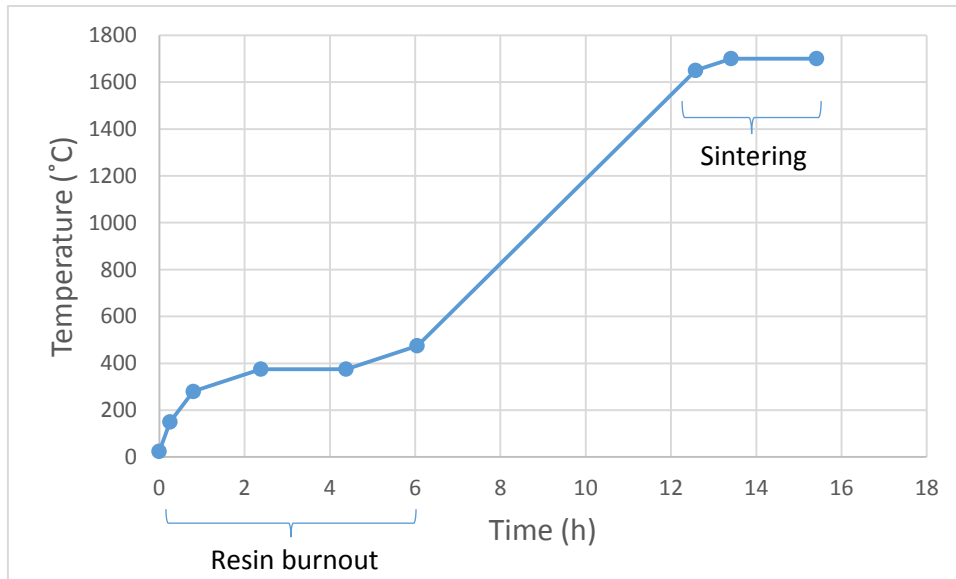


Fig 4: Sintering Cycle for Thoria Cubes including Resin Burnout Step

Pre- and post-sintering dimensional measurements of the x, y and z dimensions of the cubes were made using Vernier calipers. The sintered density was measured by the immersion method. Surface roughness measurements were done using a portable surface roughness tester, and the bulk microstructure of one of the sintered cubes was examined using optical microscopy.

### 3. Results and Discussion:

The 3D printed thorium dioxide cubes, pre- and post-sintering, are shown in Figure 5. The freshly-printed cubes appeared to have rough surfaces. The sintered parts had a similar appearance. Some of the larger bumps that can be seen in the finished part are due to incomplete removal of the support structure which contacted the cubes with a spot diameter of 0.2 mm. Surface roughness measurements were taken in different directions along the edges of the sintered cubes. The measurements varied from 4 to 7  $\mu\text{m Ra}$  (roughness arithmetic mean) with most measurements falling between 4-5  $\mu\text{m Ra}$ . The reason for the differences in measurements was due to the orientation of the measurement path in relation to the build lines of the cube. Studies on other dense ceramic parts, which were prepared in a similar manner, reported a threefold increase in the surface roughness when comparing measurements along the plane of an individual layer with those taken perpendicular to the individual layers (i.e. the build direction) [5]. The surface roughness of the sintered parts exceeds specifications for nuclear fuels. The current process needs improvement to yield a smoother surface finish or a post-sintering surface treatment would be required.

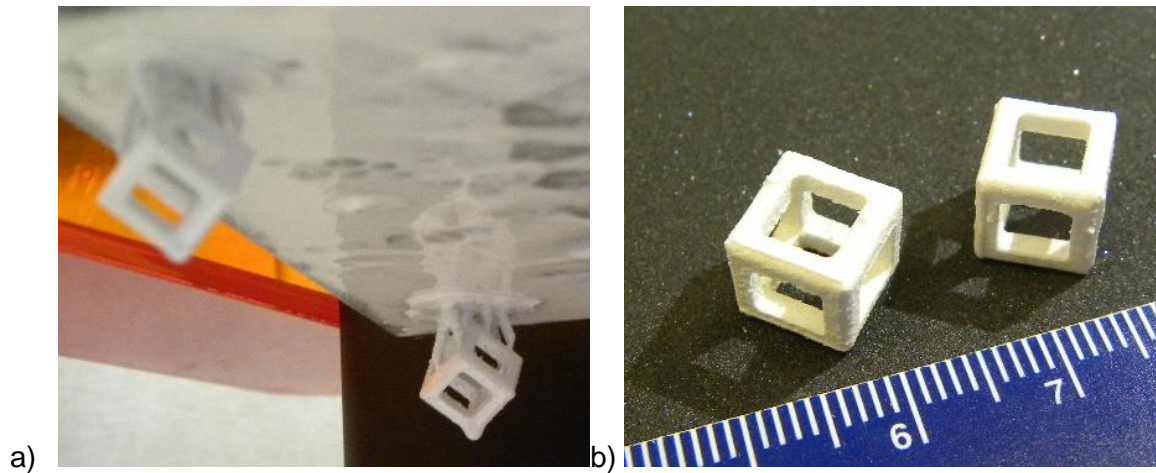


Fig 5: Picture of Thoria Cubes a) After printing b) After support removal and sintering

Table 1 provides the measured pre- and post-sintered dimensions of the cubes, as well as their measured immersion densities. The measured dimensions of the printed cubes were slightly larger than the dimensions of the 3D model with a maximum measured deviation of about 3%. Linear shrinkage during sintering was in the range of 18-23%. Achieved sintered densities were about 90% of theoretical density for both cubes 1 and 2. The printing process is able to achieve acceptable dimensional accuracy. However, the sintering process caused slight distortion in the shape of the cubic objects. If the distortion is found to be reproducible, it may be possible to compensate by changing the 3D model so that the sintered part results in the desired shape. Great care must be put into developing the printing and sintering processes together to avoid warping of the finished part.

Typical densities for nuclear fuel are greater than 95% of theoretical density (compared to ~90% for these trials). Although not investigated in the present study, it is expected that reformulation of the resin mixture will likely lead to higher sintered part densities. This is hypothesized because a similar 3D-printing process using alumina has been shown to produce parts with sintered densities in excess of 99% theoretical density [5].

Cube	Measurement taken	X dimension (mm)	Y dimension (mm)	Z dimension (mm)	Sintered density (g/cm <sup>3</sup> )	% Theoretical
1	Pre-sintering	10.15	10.24	10.22	9.168	91.7
	Post-sintering	8.31	8.34	8.41		
2	Pre-sintering	10.12	10.31	10.15	8.971	89.7
	Post-sintering	7.95	7.98	7.97		

Tab 1: Measured Dimensions and Densities of 3D-Printed Thoria Cubes

Post-sintering, one of the cubes was mounted in resin and sectioned along one of its square faces. The cut surface was ground and polished for examination by optical microscopy. A digital microscope system was used to capture and stitch images of the polished surface. A composite image is provided in Figure 6. The layered structure of the cube is apparent in the top left corner of the image. There appear to be some small cracks (see arrows) throughout the structure that run parallel and normal to the build lines in the top left corner. These cracks may have been formed during heating (resin burnout and sintering) if there was trapped, uncured resin monomers in the green (unsintered) part. Cracks such as these have been reported in silica ceramics that were prepared in a similar manner (polymeric stereolithography). The cracking was attributed to strains arising from shrinkage due to thermally-induced polymerization of residual monomer on heating [5].

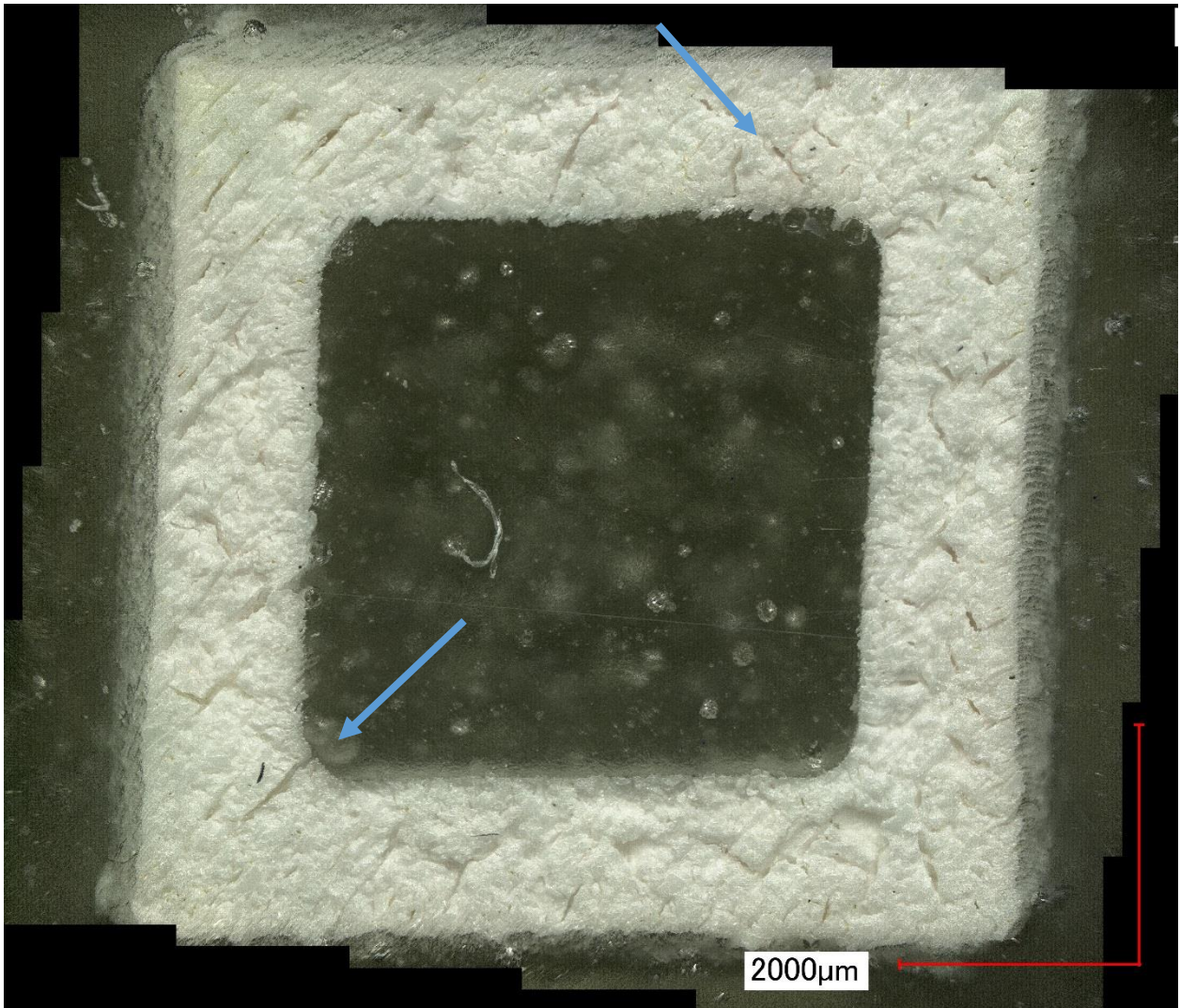


Fig 6: Composite Cross-sectional Image of a 3D Printed Cube Face. Arrows indicate cracks parallel and normal to build lines.

Impurities analysis of the starting thorium dioxide material and material that was printed and sintered is provided in Table 2. As can be seen, there is no increase in the amounts of carbon or tin. In fact, there is less carbon in the printed and sintered thorium dioxide material than the starting powder. This provides confidence that the resin material is removed from the sintered parts.

Starting Thoria Powder*		3D-Printed Material Following Sintering	
Element	Concentration ( $\mu\text{g/g}$ )	Element	Concentration ( $\mu\text{g/g}$ )
C	4.60E+02	C	<1.1E+01
Cr	5.0 $\pm$ 0.6	Sn	<0.7
La	0.15 $\pm$ 0.03		
Ce	0.15 $\pm$ 0.03		
Nd	0.22 $\pm$ 0.03		
Sm	0.09 $\pm$ 0.03		
U	56 $\pm$ 3		

\*Powder was also analyzed for Be, B, Na, Mg, Al, Ti, V, Mn, Fe, Co, Ni, Cu, Zn, Ga, Ge, As, Se, Rb, Sr, Zr, Nb, Mo, Ru, Rh, Pd, Ag, Cd, Sn, Sb, Te, Cs, Ba, Pr, Eu, Gd, Dy, Er, Tm, Yb, Lu, Hf, Ta, W, Re, Ir, Pt, Au, Tl, Pb, however, the concentrations of these elements were less than the detection limit of the ICP-MS instrument

Tab 2: Impurities Analysis of Starting Thoria Powder and 3D-Printed Material Following Sintering

The process that was employed in these preliminary trials was relatively slow requiring approximately 3.5 hours to make two small parts. While a larger number of parts could have been printed simultaneously with a non-linear increase in the print time, this process would not be feasible for application to large scale nuclear fuel production. However, similar, faster 3D-printing technologies are being developed that could be applied to make the same parts. For example, a recent study described one-step volumetric additive manufacturing of complex polymer structures from photosensitive resins using holographic light fields [6]. The parts were manufactured in seconds (as opposed to hours) resulting in production times comparable to conventional nuclear fuel manufacturing.

#### 4. Summary and Conclusions

Additive manufacturing was applied successfully to nuclear fuel material using a consumer-grade 3D printer and commercially available photocurable resin. Thorium dioxide was printed and sintered to densities of ~90% of theoretical density without addition of impurities from the resin used in the stereolithography process. Improvements still need to be made to the process to increase the sintered density of the printed parts, decrease the surface roughness, and mitigate non-uniform distortion during sintering. This study shows the potential for using additive manufacturing for fabrication of nuclear fuel materials with complex geometries. Without the geometric constraints of conventional fuel manufacturing, fuel designers may be able to devise fuel geometries optimized for improved fuel performance and safety.

#### 5. Acknowledgements

The authors thank Clinton Mayhew for the SEM image of the thoria powder, Al Lockley for the composite image of the thoria cube face, and Julie Pring and Roxanne Collins for chemical analysis. This study was funded by Atomic Energy of Canada Limited.

#### 6. References

[1] Bourell, D. et al. "Materials for Additive Manufacturing", CIRP- Annals- Manufacturing Technology (2017)

[2] M.A. Pouchon, M. Streit, "3D Ceramic Printing of Nuclear Fuel", Paul Scherrer Institute, PSI REPORT TM-46-16-04, Switzerland, 2016.



- [3] Zocca, A., Colombo, P., Gomes, C.M., Günster, J., "Additive Manufacturing of Ceramics: Issues, Potentialities, and Opportunities, J. Am. Ceram. Soc., 98 (7) 1983-2001, July 2015.
- [4] Griffith, M.L., Halloran, J.W., "Freeform Fabrication of Ceramics via Stereolithography", J. Am. Ceram. Soc., 79 (10) 2601-2608, October 1996.
- [5] Schwentenwein, M. Homa, J., "Additive Manufacturing of Dense Alumina Ceramics", Int. J. Appl. Ceram. Technol., 12 (1) 1-7, January 2015.
- [6] Shusteff, M., Browar, A.E.M., Kelly, B., Henriksson, J., Weisgraber, T.H., Panas, R.M., Fang, N.X., Spadaccini, C.M., "One-step Volumetric Additive Manufacturing of Complex Polymer Structures", Science Advances, 3 (12) eaao5496, December 2017.